Frontiers in Bioscience Landmark

Front. Biosci. (Landmark Ed) **2026**; 31(11): 57602
https://doi.org/10.31083/FBL57602

Original Research

Nanobody-Mediated Retargeting of SpyTag/SpyCatcher-Based Universal CAR-T Cells Against CD22-Positive Burkitt Lymphoma Cells

Amirhosein Maali[1,2], Shahriyar Abdoli[3], Mahdi Habibi-Anbouhi[4], Ahmad Noei[1], Mahdieh Jafari[1], Arash Arashkia[5,*], Zahra Sharifzadeh[1,*]

[1]Department of Immunology, Pasteur Institute of Iran, 13169-43551 Tehran, Iran
[2]Department of Medical Biotechnology, Faculty of Allied Medicine, Qazvin University of Medical Sciences, 34197-59811 Qazvin, Iran
[3]School of Advanced Medical Technologies, Golestan University of Medical Sciences, 49189-36316 Gorgan, Iran
[4]National Cell Bank, Pasteur Institute of Iran, 13169-43551 Tehran, Iran
[5]Department of Molecular Virology, Pasteur Institute of Iran, 13169-43551 Tehran, Iran
*Correspondence: arash.arashkia@gmail.com (Arash Arashkia); zsharifzadeh@gmail.com (Zahra Sharifzadeh)
Academic Editor: Christian Borgo
Submitted: 31 August 2026 Revised: 21 October 2026 Accepted: 26 October 2026 Published: 19 November 2026

Abstract

Background: Conventional chimeric antigen receptor (CAR)-T-cell therapies are typically restricted to a single tumor antigen and may lose efficacy following antigen escape. Modular CAR platforms separate antigen recognition from T-cell signaling and may enable flexible redirection of a single engineered T-cell product. SpyCatcher is a protein domain that spontaneously forms a stable covalent isopeptide bond with its cognate SpyTag peptide, providing a robust interface for post-translational receptor assembly. This study aimed to develop a SpyTag/SpyCatcher-based universal CAR-T-cell system redirected against CD22-expressing cells using a SpyTag-fused anti-CD22 nanobody. **Methods:** A second-generation SpyCatcher-based CAR, comprising CD28 transmembrane and intracellular costimulatory domains and a CD3ζ signaling domain, was constructed and introduced into primary human T cells using a lentiviral vector. A SpyTag-fused anti-CD22 nanobody was used as the targeting module (TM). CAR expression, TM binding, T-cell activation, proliferation, cytokine secretion, and cytotoxicity against CD22-positive ($CD22^+$) Raji Burkitt lymphoma cells were evaluated using flow cytometry and enzyme-linked immunosorbent assay (ELISA). CD22-negative ($CD22^-$) K562 cells and mock-transduced T cells were used as controls. All functional experiments included three within-donor experimental replicates from a single healthy donor (n = 3; N = 1 donor). **Results:** Structural superimposition demonstrated preservation of the predicted SpyCatcher conformation within the CAR construct, with a root-mean-square deviation (RMSD) of 1.109 Å. Lentiviral transduction resulted in 39.5% GFP-positive cells, and SpyCAR surface expression was detected in 29.0% of transduced cells. The TM bound to 16.1% of GFP-positive (SpyCAR-transduced) cells. In the presence of $CD22^+$ target cells, 10 nM TM induced CD69 expression in 64.1% of SpyCAR-T cells and increased CD25 expression to 13.5%. SpyCAR-T cells also showed enhanced Ki-67 expression and produced high levels of interleukin-2 (IL-2) and interferon-gamma (IFN-γ), reaching 2506 ± 91.43 pg/mL and 1777 ± 75.55 pg/mL, respectively. At an effector-to-target ratio of 3:1, 49.7% of CD3-negative target cells were 7-AAD-positive, indicating substantial cytotoxic activity. **Conclusion:** The SpyTag/SpyCatcher-based SpyCAR platform demonstrated T-cell activation, proliferation-associated responses, cytokine secretion, and preliminary cytotoxic activity against $CD22^+$ Raji Burkitt lymphoma cells *in vitro*. These findings support further development of this modular system as a flexible strategy for retargetable CAR-T-cell therapy. However, no direct comparisons with a conventional anti-CD22 CAR, a noncovalent adaptor CAR, or a bond-deficient SpyTag/SpyCatcher control were performed; therefore, comparative efficacy and the specific contribution of covalent coupling remain unestablished.

Keywords: receptors, chimeric antigen; single-domain antibodies; Sialic Acid Binding Ig-like Lectin 2; immunotherapy, adoptive

1. Introduction

CD22, a sialic acid-binding Ig-like lectin (Siglec) prominently expressed on mature B cells, plays a crucial role in B-cell receptor signaling by acting as a checkpoint that modulates immune responses [1]. This protein is vital for the development and maintenance of normal B-cell function. Its selective expression on B cells and involvement in their activation and survival make CD22 an attractive target for immunotherapy strategies aimed at B-cell malignancies, including certain leukemias and lymphomas. Chimeric antigen receptor (CAR)-T cell therapies targeting CD22 have demonstrated promising results in clinical trials, particularly for treating relapsed or refractory B-cell malignancies. These therapies involve engineering T cells to express a CAR that recognizes CD22 and directs them to eliminate CD22-expressing cells [2].

Antigen escape is a major mechanism of resistance in which cancer cells lose or alter the targeted antigen [3]. Multi-targeting also enhances the potency and applicability of CAR-T cell therapy across different patient populations and tumor types. Utilizing the SpyTag/SpyCatcher system in CAR-T cell engineering offers the potential for a 'uni-

Copyright: © 2026 The Author(s). Published by IMR Press.
This is an open access article under the CC BY 4.0 license.

Publisher's Note: IMR Press stays neutral with regard to jurisdictional claims in published maps and institutional affiliations.

versal' CAR-T platform where different targeting modules (TM) can be quickly and robustly attached to effector cells [4].

The SpyTag/SpyCatcher system represents a significant advancement in molecular engineering, particularly for CAR-T cell therapy, by enabling stable, covalent linkage of proteins. This system operates through a small peptide, SpyTag, and its partner protein, SpyCatcher, which form a strong isopeptide bond, facilitating modular protein assembly [5]. This feature is crucial in CAR-T cell therapy, where adaptability to diverse and changing tumor antigens is necessary. The flexibility of the SpyTag/SpyCatcher system allows for easy selection of antigen-specific TMs on CARs, enabling rapid redirection of T cells to various tumor markers [4]. This is essential for managing tumors that alter their antigen expression to evade immune responses. The covalent bond ensures that these TMs are permanently attached, enhancing the stability and long-term efficacy of CAR-T cells. This system also opens possibilities for multi-antigen targeting, which could be more effective against heterogeneous tumors and help in preventing antigen escape [6].

Nanobodies, also known as VHH single-domain antibodies, are particularly well suited for use as TMs in modular CAR platforms. Compared with conventional monoclonal antibodies and single-chain variable fragments, nanobodies have a compact single-domain structure, high solubility and biochemical stability, and can be efficiently produced and genetically modified in microbial expression systems [7]. Their small molecular size may reduce the steric burden imposed on the receptor–target interface and facilitate access to membrane-proximal or spatially restricted epitopes, while their simple architecture enables straightforward fusion to molecular tags, linkers, and additional binding domains. These characteristics allow nanobodies to be rapidly converted into interchangeable, multivalent, or multispecific TMs without redesigning the intracellular signaling receptor [8]. In universal CAR systems, nanobody-based modules may therefore support flexible antigen switching, simultaneous or sequential multi-antigen targeting, and optimization of receptor geometry and antigen sensitivity. However, their relatively rapid systemic clearance and potential immunogenicity should be considered during translational development and may require half-life extension or humanization strategies [9,10]. The aim of this study is to design and construct SpyTag/SpyCatcher-based universal CAR-T cells capable of being retargeted against CD22-expressing Raji Burkitt lymphoma cells. The innovative approach promises to enhance the adaptability and efficacy of CAR-T cell therapy for B-cell malignancies.

2. Materials and Methods

2.1 Sample Preparation

Peripheral blood samples were obtained from a healthy donor and processed in accordance with the approved institutional protocol.

2.2 Cell Lines and Cultures

LentiX-293T and HEK-293T cells, obtained from the Pasteur Institute of Iran, were used for lentiviral particle production and titration, respectively. Both cell lines were maintained in Dulbecco's modified Eagle medium (DMEM; Biosera, France) supplemented with 10% fetal bovine serum (FBS; FB-1001, BioSera, Cholet, France), and penicillin (100 IU/mL)-streptomycin (100 µg/mL) (15140122, Gibco, Grand Island, NY, USA). Raji (a human Burkitt lymphoma cell line) and K562 (a human chronic myeloid leukemia cell line), obtained from the Pasteur Institute of Iran, were used as $CD22^+$ and $CD22^-$ target cells, respectively. These cells were maintained in RPMI-1640 medium (LM-R1640/500, BioSera, Cholet, France) supplemented with 10% FBS, 100 IU/mL penicillin, and 100 µg/mL streptomycin. Human peripheral blood mononuclear cells (PBMCs) were cultured in RPMI-1640 medium supplemented with 10% FBS, 100 IU/mL penicillin, 100 µg/mL streptomycin, and 100 IU/mL recombinant human interleukin-2 (IL-2; Royan Biotechnology Center, Iran). All cells were maintained at 37 °C in a humidified atmosphere containing 5% CO_2. The identity of the cell lines was verified by short tandem repeat (STR) profiling, and all cell lines were confirmed to be negative for mycoplasma contamination prior to their acquisition, as documented in the authentication and quality control records provided by the cell bank.

2.3 Design of the SpyCAR and TM Constructs

A second-generation universal CAR, designated SpyCAR, was designed by replacing the conventional antigen-binding domain with SpyCatcher. The SpyCAR expression cassette comprised an N-terminal signal peptide, an extracellular c-Myc epitope tag, the SpyCatcher domain, a CD28-derived hinge and transmembrane domain, the CD28 intracellular costimulatory domain, and the CD3ζ signaling domain. A self-cleaving 2A peptide followed by green fluorescent protein (GFP) was included downstream of the CAR sequence to enable identification of successfully transduced cells.

The TM was designed to contain an anti-CD22 (aCD22) nanobody at its N-terminus, followed by a $[G_4S]_4$ linker, SpyTag, an HA epitope tag, and a C-terminal His tag. This protein was generated and evaluated in our previous study [11].

2.4 Computational Modeling and Structural Assessment

Before gene synthesis and molecular cloning, the potential effect of incorporating SpyCatcher into the com-

plete SpyCAR architecture was evaluated computationally. The amino acid sequences of free SpyCatcher and the designed SpyCAR construct were separately submitted to the I-TASSER server for three-dimensional structure prediction. For each sequence, the model with the highest confidence score was selected and subsequently refined using the GalaxyRefine server.

The refined structure of free SpyCatcher was then superimposed onto the corresponding SpyCatcher region within the complete SpyCAR model using UCSF Chimera version 1.18. Structural similarity was assessed by calculating the root-mean-square deviation between the aligned structures. This analysis was performed to determine whether integration of SpyCatcher into the CAR architecture was predicted to cause substantial conformational alteration of the extracellular binding domain.

2.5 Synthesis and Molecular Cloning of the SpyCAR Construct

Following completion of the construct design and computational structural assessment, the c-Myc-SpyCatcher coding sequence was synthesized by GeneScript, China, and supplied in the pUC57 plasmid. The synthesized sequence was excised from pUC57 and subcloned into a pBluescriptSK-based second-generation CAR backbone using the *Pst*I and *EcoR*V restriction sites. The recipient CAR backbone contained the CD28 hinge, CD28 transmembrane and intracellular costimulatory domains, and the CD3ζ signaling domain.

The resulting pBluescriptSK-SpyCAR construct was verified by restriction enzyme digestion. The complete SpyCAR expression cassette was subsequently excised using *BamH*I and *Not*I and subcloned into the pCDH lentiviral transfer vector. The reporter configuration was modified to generate the final SpyCAR-2A-GFP expression cassette. The integrity and orientation of the final pCDH-SpyCAR construct were confirmed by restriction enzyme analysis and Sanger sequencing. Also, a pCDH construct (GFP only, without SpyCAR) was used as mock.

2.6 Lentiviral Production and Titration

To produce the SpyCatcher-CAR-encoding lentivirus, the recombinant pCDH, pMD2.G and psPAX2 plasmids were co-transfected into the LentiX-293T cells. Briefly, 1.2×10^6 cells per well were seeded in a six-well plate and transfected using a total of 4.5 µg of plasmid DNA and 9 µL of polyethylenimine (PEI). After 16 h, the supernatant was removed; then, the virus-containing crude supernatants were collected for 72 h (replaced with fresh medium each 12 h). Different volumes of viral suspension (10–500 µL), adjusted to a final volume of 500 µL with culture medium, were added to HEK-293T cells seeded at 5×10^4 cells per well in a 24-well plate to determine the viral titer.

2.7 Lentiviral Transduction of PBMCs and Immunophenotyping

PBMCs were isolated from a single healthy donor using Lymphosep (LM-T1702/500, BioSera, Cholet, France), according to the manufacturer's instructions. All functional assays used cells derived from this donor. The isolated PBMCs were considered for activation by human T cell activation/expansion kit (130-091-441, Miltenyi Biotec, Bergisch Gladbach, Germany) containing CD2/CD3/CD28-coated magnetic beads. After 72 h incubating of PBMCs with antibody-coated beads at 37 °C and 5% CO_2, the activated T cells were separated by magnetic cell sorting. Then, the magnetic beads were removed from the sorted cells; the isolated T cells were incubated for 24 h at 37 °C and 5% CO_2. Then, T cells were transduced by recombinant viral particles by MOI = 2. After 24 h, virus-containing media were removed and cells were cultured for 48 h in fresh media. The percentage of GFP^+ cells measured by flow cytometry was used to determine lentiviral transduction efficiency.

The immunophenotyping was performed on transduced T cell population in terms of $CD3^+$ and $CD4^+$. In brief, 1×10^6 transduced and non-transduced cells were resuspended in 100 µL staining buffer (phosphate-buffered saline (PBS) containing 2% FBS) containing PE-conjugated anti-CD3 (10 µL, R0810, Dako Glostrup, Denmark) and PerCP-Cy5.5-conjugated anti-CD4 (5 µL, 45-0049-42, eBioscience/Thermo Fisher Scientific, San Diego, CA, USA) antibodies. After washing, cells were subjected to flow cytometry. The main cell population was initially identified based on FSC/SSC characteristics, followed by singlet discrimination to exclude cell aggregates. CD3 and CD4 expression were then simultaneously analyzed using quadrant gating to distinguish $CD3^+CD4^+$, $CD3^+CD4^-$, $CD3^-CD4^+$, and $CD3^-CD4^-$ populations, as illustrated in **Supplementary Fig. 1**.

2.8 Evaluation of SpyCAR Cell-Surface Expression

Cell-surface expression of SpyCAR was evaluated by detecting the extracellular c-Myc epitope tag located at the N-terminus of the receptor. Seventy-two hours after lentiviral transduction, 1×10^6 SpyCAR-transduced or mock-transduced PBMCs were harvested and resuspended in 100 µL of staining buffer consisting of phosphate-buffered saline supplemented with 2% FBS. Cells were incubated with PerCP-Cy5.5-conjugated anti-c-Myc antibody (2 µL, sc-40 PCPC5, Santa Cruz Biotechnology, Dallas, USA) for 45 min at 4 °C in the dark. Following incubation, the cells were washed twice with wash buffer and analyzed by flow cytometry.

2.9 Evaluation of TM Binding to Cell-Surface SpyCAR

For evaluating the binding capacity of the expressed SpyCAR to TM, 1×10^6 transduced PBMCs were resuspended in 100 µL staining buffer and treated with 10 nM

TM for 1 h at 4 °C. Following two washing steps, cells were treated with MonoRab™ Rabbit anti-camelid V_{HH} antibody (1 µL, A01860, GenScript, Piscataway, NJ, USA) for 45 min at 4 °C. After washing, cells were treated with PE-conjugated donkey anti-Rabbit IgG antibody (1 µL, 406421, BioLegend, San Diego, CA, USA) for 45 min at 4 °C. Then, cells were washed and considered for flow cytometry analysis. Following FSC/SSC-based cell selection and singlet gating, TM binding was assessed by evaluating PE-positive cells within the GFP-positive population.

2.10 T Cell Activation Assay

First, the suitable concentration of TM for activation of SpyCAR-T cells was determined by evaluating early activation marker, CD69, in 3:1 effector to target (E:T) ratio. To this end, 3×10^6 SpyCAR-T cells cocultured with 1×10^6 $CD22^+$ Raji cells were treated with various concentrations of TM (1 to 1000 nM). After 18 h, 1×10^6 cells were resuspended in 100 µL staining buffer and treated with PE-conjugated anti-CD69 antibody (1 µL, 310906, BioLegend, San Diego, CA, USA) for 45 min at 4 °C. After washing, the cells were analyzed by flow cytometry. Also, late activation response was evaluated in different treatment groups. For this purpose, CAR-T cells were cocultured with target cells in E:T ratio of 3:1 in the presence of 10 nM TM. After 24 h, 1×10^6 cells were resuspended in 100 µL staining buffer and treated with PE-conjugated anti-CD25 antibody (1 µL, 302606, BioLegend, San Diego, CA, USA) for 45 min at 4 °C. After washing, the cells were analyzed by flow cytometry. Following FSC/SSC-based cell selection and singlet gating, CD69 and CD25 expression were evaluated within the GFP-positive effector-cell population.

2.11 Proliferation Assay

The proliferation rate of CAR-T cells in the presence of TM and target cells was measured by evaluating the intracellular expression of Ki-67 protein. To this aim, CAR-T cells were cocultured with 10 nM TM and target cells in E:T ratio of 3:1. After 48 h, 1×10^6 cells were fixed and permeabilized using 1% (v/v) paraformaldehyde and 30% (v/v) ethanol. Then, cells were resuspended in 100 µL staining buffer and treated with PE-conjugated anti-Ki-67 antibody (1 µL, 350504, BioLegend, San Diego, CA, USA) for 45 min at 4 °C. After washing, the cells were analyzed by flow cytometry. Following FSC/SSC-based cell selection and singlet gating, Ki-67 expression was evaluated within the effector-cell population using mean fluorescence intensity (MFI).

2.12 Cytotoxicity Assay

7-AAD staining was used to evaluate the cytotoxic activity of CAR-T cells against target cells. In brief, CAR-T cells were cocultured with target cells at different E:T ratios (1:1, 3:1, and 10:1) for 24 h in the presence of TM. Cells were then collected, resuspended in 100 µL staining buffer and treated with FITC-conjugated anti-CD3 antibody (2 µL, F0818, Dako, Glostrup, Denmark) and 7-AAD (1 µg, 420403, BioLegend, San Diego, CA, USA). Target cell lysis was subsequently assessed by quantifying the percentage of $7\text{-}AAD^+$ dead cells within $CD3^-/GFP^-$ cell population using flow cytometry. Following the initial selection of the cell population based on FSC and SSC characteristics, $CD3^-/GFP^-$ events were gated to identify the target-cell-enriched population. The percentage of $7\text{-}AAD^+$ cells was calculated by dividing the number of $7\text{-}AAD^+$ events within the $CD3^-/GFP^-$ gate (target cells) by the total number of events in the same gate.

2.13 Cytokine Secretion Assay

The secreted IL-2 and interferon-gamma (IFN-γ) were measured by enzyme-linked immunosorbent assay (ELISA). For this purpose, CAR-T cells and target cells were cocultured at an E:T ratio of 3:1 for 48 h. The supernatants were then harvested and the concentrations of IL-2 and IFN-γ were measured using Human IL-2 and IFN-γ Quantikine ELISA kits (D2050 and DIF50C, respectively, R&D Systems, Minneapolis, MN, USA) according to the manufacturer's protocol.

2.14 Statistical Analysis

Data were analyzed using GraphPad Prism version 8.3 (GraphPad Software, San Diego, CA, USA). All functional experiments were performed in three separate experimental runs using cells derived from a single healthy donor (n = 3 experimental runs per condition; N = 1 donor). These runs represent within-donor experimental replication rather than independent donor-level biological replication. Data are presented as mean ± standard deviation (SD) across the three runs. Comparisons among experimental conditions were performed using ordinary one-way analysis of variance (ANOVA) followed by Tukey's multiple comparisons test. Adjusted p-values < 0.05 were considered statistically significant. Statistical inference was restricted to within-donor experimental comparisons and does not establish generalizability across donors. Flow cytometry data were analyzed using FlowJo version 10 (FlowJo LLC, Ashland, OR, USA).

3. Results

3.1 SpyCAR Construction, Transduction, Surface Expression, and Binding to TM

The SpyCAR construct was designed to incorporate the SpyCatcher as a universal extracellular domain, followed by the CD28 transmembrane and intracellular signaling domains, and CD3ζ activation domains (Fig. 1A). A TM containing an aCD22-nanobody at the N-terminus and a SpyTag at the C-terminus was utilized for the engagement of SpyCAR with $CD22^+$ target cells (Fig. 1B). The predicted SpyCatcher structure was superimposed onto the corresponding region of the predicted SpyCAR structure to

assess structural similarity. Structural superimposition using UCSF Chimera yielded an RMSD of 1.109 Å, indicating high structural overlap and no significant conformational changes in the SpyCatcher protein model upon incorporation into the SpyCAR construct (Fig. 1C,D). Following the construction of the pCDH-SpyCAR plasmid, lentiviral particles were produced by plasmid co-transfection of LentiX-293T cells, with a GFP-based transfection efficiency of 97.2% (Fig. 1E). Also, surface expression of CD22 on Raji cells evaluated by flow cytometry was 85.6%, while for negative control (K562 cells) it was 0.74% (Fig. 1F).

Following harvesting and titration of the recombinant lentiviral particles, PBMCs were transduced at an MOI of 2. After 72 h, the percentage of GFP^+ cells was 39.5%, representing the transduced population (Fig. 1G). The surface expression of SpyCAR was evaluated by flow cytometry using an anti-c-Myc antibody. The results show that 29.0% of cells were positive for SpyCAR, whereas mock cells are negative for surface expression of c-Myc, containing a slight background for binding (Fig. 1H). Also, flow cytometry analysis showed that 16.1% of GFP^+ cells were positive for TM binding (Fig. 1I), indicating significant TM binding of TM to SpyCAR.

3.2 Activation of SpyCAR-T Cells in the Presence of TM

To determine the optimum concentration of TM for activating SpyCAR-T cells, SpyCAR-T cells were co-cultured with $CD22^+$ target cells in the presence of different concentrations of TM. The positivity of CD69 was 64.1% at 10 nM TM and increased further at higher tested concentrations; therefore, 10 nM was selected as the working concentration rather than an established optimal dose (Fig. 2A). We also found that the positivity of CD25-expressing cells was modestly higher in the complete SpyCAR-T/Raji/TM condition (13.5%) than in the control conditions (4.39–5.95%), suggesting a TM-associated activation response under the tested conditions (Fig. 2B).

3.3 Cytotoxicity of SpyCAR-T Cells Against Target Cells

7-AAD staining was used to evaluate the cytotoxic effect of SpyCAR-T cells on target cells in the presence of TM. For this purpose, SpyCAR-T cells and target cells were cocultured at different E:T ratios for 24 h in the presence of 10 nM TM. At an E:T of 3:1, 49.70 ± 3.75% of $CD3^-$ cells were 7-AAD^+. Although the proportion of 7-AAD^+CD3^- cells increased at an E:T ratio of 10:1 (52.37 ± 6.53%), the difference was not statistically significant (Fig. 3A). Therefore, an E:T ratio of 3:1 was selected as the optimal ratio for subsequent assays. Three experimental runs were performed using cells from a single healthy donor, representing within-donor replicates.

3.4 Proliferation and Cytokine Secretion of SpyCAR-T Cells

SpyCAR-T cells were capable of secreting cytokines and proliferating in the presence of target cells and TM. After 48 h of co-culture, cells were stained with Ki-67 to evaluate SpyCAR-T cell proliferation. The relative MFI results showed a significant increase in Ki-67 intensity in SpyCAR-T cells in the presence of $CD22^+$ target cells and TM (1865 ± 153.1) compared to control co-culture groups (890.7 ± 83.01 for mock control, 795.3 ± 60.34 for control group without TM, 795.0 ± 143.5 for non-specific target control; $p < 0.0001$ for all groups). (Fig. 3B). Additionally, the culture supernatants were collected to quantify IL-2 and IFN-γ secretion via ELISA. In the presence of $CD22^+$ target cells and TM, SpyCAR-T cells secreted significantly higher levels of IL-2 and IFN-γ (2506 ± 91.43 pg/mL and 1777 ± 75.55 pg/mL, respectively), whereas cytokine secretion remained negligible in the control groups ($p < 0.0001$ for all groups) (Fig. 3C).

3.5 Immunophenotyping of SpyCAR-T Cells

Immunophenotyping of T cells was performed by evaluating CD3 and CD4 expression at three distinct time points: immediately following PBMC isolation, after T cell activation with antibody-coated magnetic beads, and 72 h post-lentiviral transduction with SpyCAR. As expected, the proportion of $CD3^+$ increased during the activation and transduction phases compared to PBMCs immediately after isolation. Furthermore, SpyCAR lentiviral transduction did not significantly alter the $CD4^+$:$CD3^+$ ratio compared to the post-activation stage (Fig. 3D).

4. Discussion

In this study, we developed a nanobody-based modular CAR-T cell system using the SpyTag/SpyCatcher platform for targeting CD22. SpyCAR-T cells carry a fixed SpyCatcher-CD28-CD3ζ signaling receptor, whereas antigen specificity is supplied by a nanobody-based TM. This design separates antigen recognition from T-cell signaling. SpyTag and SpyCatcher form a spontaneous covalent isopeptide bond under physiological conditions [12].

The closest conceptual comparator is the SpyCatcher immune receptor described by Minutolo et al. [4], which redirected human T cells using SpyTag-conjugated antibodies and genetically fused ligands against several tumor antigens. The present study extends this principle to $CD22^+$ Raji cells using a compact, genetically encoded nanobody-SpyTag TM. This format may simplify recombinant production and improve epitope access, but its monovalent nanobody format and the geometry imposed by the $[G_4S]_4$ linker between the nanobody and SpyTag differ from those of full antibodies. Recent studies indicate that these design parameters can influence the functional activity of SpyTag/SpyCatcher-based immune-cell platforms. Increasing SpyTag valency enhanced SpyCAR-NK92 cy-

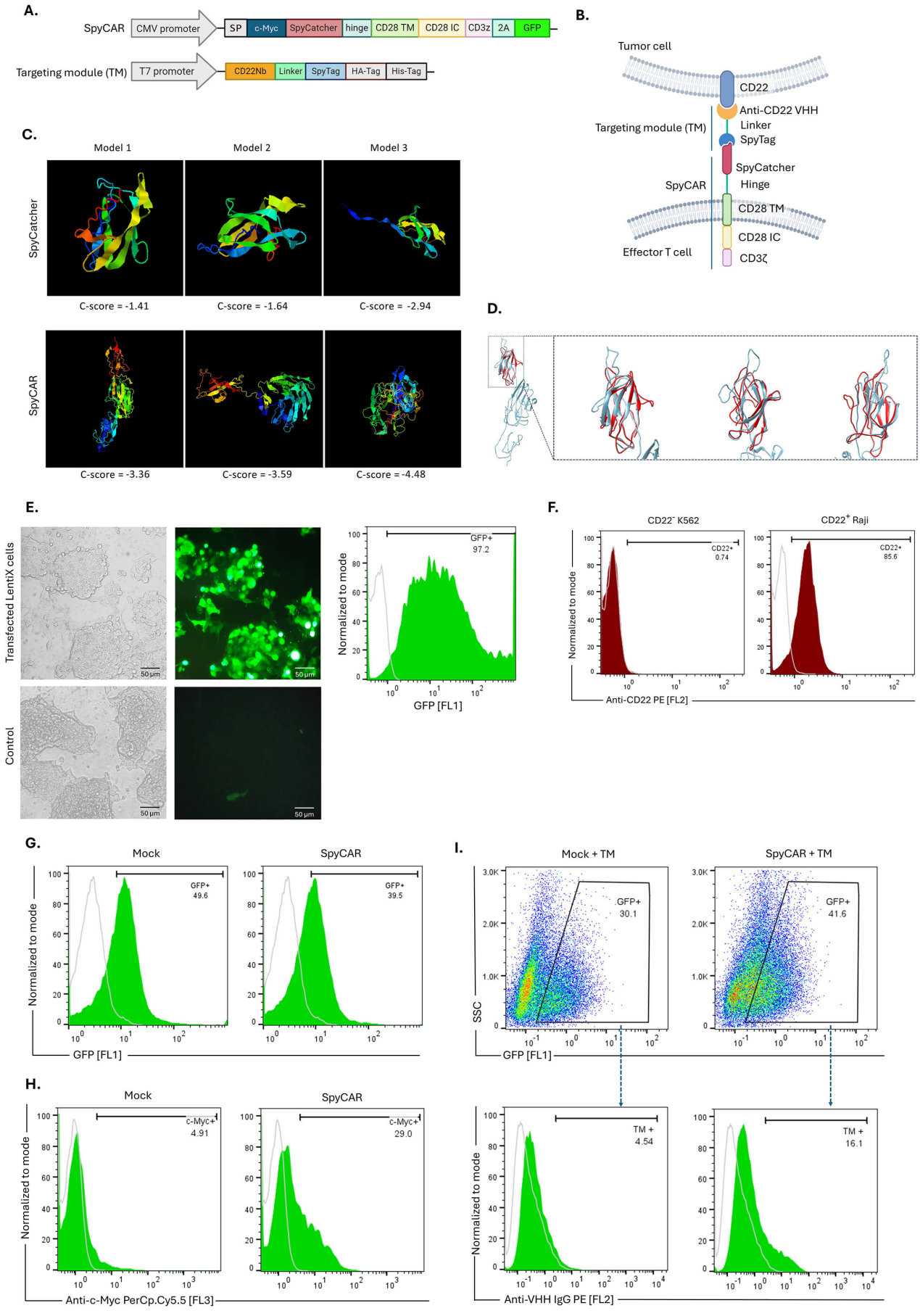

A.
SpyCAR
CMV promoter
SP
c-Myc
SpyCatcher
hinge
CD28 TM
CD28 IC
CD3z
2A
GFP
Targeting module (TM)
T7 promoter
CD22Nb
Linker
SpyTag
HA-Tag
His-Tag
B.
Tumor cell
CD22
Anti-CD22 VHH
Linker
SpyTag
Targeting module (TM)
SpyCatcher
SpyCAR
Hinge
CD28 TM
CD28 IC
Effector T cell
CD3ζ
C.
Model 1
Model 2
Model 3
SpyCatcher
C-score = -1.41
C-score = -1.64
C-score = -2.94
SpyCAR
C-score = -3.36
C-score = -3.59
C-score = -4.48
D.
E.
Transfected LentiX cells
Control
50 μm
GFP+
97.2
Normalized to mode
GFP [FL1]
F.
CD22⁻ K562
CD22⁺ Raji
CD22+
0.74
CD22+
85.6
Normalized to mode
Anti-CD22 PE [FL2]
G.
Mock
SpyCAR
GFP+
49.6
GFP+
39.5
Normalized to mode
GFP [FL1]
H.
Mock
SpyCAR
c-Myc+
4.91
c-Myc+
29.0
Normalized to mode
Anti-c-Myc PerCp.Cy5.5 [FL3]
I.
Mock + TM
SpyCAR + TM
GFP+
30.1
GFP+
41.6
SSC
GFP [FL1]
TM +
4.54
TM +
16.1
Normalized to mode
Anti-VHH IgG PE [FL2]

Fig. 1. Construction, development and validation of SpyCAR. (A) Schematic representation of the SpyCAR and TM constructs. The second-generation SpyCAR consisted of a signal peptide (SP), an extracellular SpyCatcher domain, a hinge region, the CD28 transmembrane and intracellular costimulatory (IC) domains, and the CD3ζ signaling domain, followed by a self-cleaving 2A peptide and green fluorescent protein (GFP) reporter. The TM comprised an anti-CD22 nanobody connected through a flexible linker to SpyTag, followed by HA- and His-tags. (B) Schematic illustration of the modular targeting mechanism. The anti-CD22 nanobody portion of the TM recognizes CD22 expressed on the tumor-cell surface, whereas SpyTag covalently engages the extracellular SpyCatcher domain of SpyCAR expressed on the effector T cell, thereby bridging the effector and target cells. (C) Three-dimensional structural models of SpyCatcher and the complete SpyCAR construct predicted using the I-TASSER server. The three highest-ranked models generated for SpyCatcher had C-scores of –1.41, –1.64, and –2.94, whereas the corresponding SpyCAR models had C-scores of –3.36, –3.59, and –4.48. For each construct, Model 1, which had the highest C-score, was selected for subsequent refinement and structural analysis. (D) Structural superimposition of the refined SpyCatcher and SpyCAR models using UCSF Chimera, shown from multiple orientations. The SpyCatcher structure is shown in red, whereas the SpyCAR model is shown in light blue. Superimposition of the SpyCatcher region within the complete SpyCAR structure resulted in a root-mean-square deviation of 1.109 Å, indicating preservation of the predicted SpyCatcher conformation following its incorporation into the CAR architecture. (E) Representative light and fluorescence microscopy images of lentiviral producer cells following plasmid co-transfection and its non-transfected control, together with flow-cytometric analysis of GFP expression. A transfection efficiency of 97.2% was observed. Scale bars, 50 µm. (F) Cell-surface CD22 expression was evaluated using a PE-conjugated anti-CD22 antibody. CD22 expression was detected in 85.6% of Raji cells, confirming their use as the CD22-positive target-cell line, whereas only 0.74% of K562 cells were CD22-positive, supporting their use as the CD22-negative control. Colored histograms represent anti-CD22-stained cells, and the overlaid unfilled histograms represent the corresponding unstained controls. (G) Flow-cytometric assessment of PBMC transduction 72 h after exposure to the respective lentiviral vectors at a multiplicity of infection of 2. (H) Cell-surface expression of SpyCAR was evaluated by staining the extracellular c-Myc epitope. c-Myc positivity was detected in 29.0% of SpyCAR-transduced cells compared with 4.91% background staining in mock cells. (I) TM binding was assessed within the GFP^+ population. The percentages shown indicate TM positivity within this gate, rather than GFP positivity: 16.1% for GFP-positive transduced cells and 4.54% for mock cells. Gray histogram overlays represent the corresponding unstained controls. pCDH (GFP-only) construct was used as mock.

totoxicity [13], accelerated SpyCatcher003/SpyTag003 chemistry enabled *in vivo* arming of DB5 universal CAR-T cells [14], and SpyTag/SpyCatcher-assembled CAR-like NK cells retained surface engagers and antitumor activity *in vivo* [15]. Site-specific SpyTag-based switch modules have likewise expanded antigen redirection through anti-FITC CAR-T cells [6]. Thus, the present construct represents a nanobody-based application of the SpyTag/SpyCatcher modular immune-receptor approach for targeting CD22.

A key mechanistic finding was the stepwise decrease from GFP positivity of 39.5% to detectable surface SpyCAR expression of 29.0% and TM binding of 16.1%. These assays measure different biological layers. GFP reflects vector expression; extracellular c-Myc staining reflects receptor delivery to the plasma membrane; and TM detection additionally depends on SpyCatcher accessibility, receptor occupancy, TM integrity, washing, and the multistep detection method. Therefore, the lower binding fraction does not necessarily indicate receptor failure. Importantly, this fraction was sufficient to trigger substantial signaling, showing that functional output is not linearly predicted by the percentage of ligand-positive cells. Minutolo et al. [4] similarly reported dose-dependent receptor loading and reduced maximal activity when covalent bond formation was disrupted.

At 10 nM TM, 64.1% of GFP^+ SpyCAR-T cells expressed CD69. Because activation increased further at 100 and 1000 nM, 10 nM is best interpreted as the lowest tested concentration producing a strong, near-plateau response, rather than the maximally active dose. This distinction matters because TM dose is a pharmacological control variable. Noncovalent UniCAR systems show dose-dependent activity [16], and clinical UniCAR-T-CD123 data demonstrate that a rapidly cleared TM can provide an on/off mechanism [17]. Extending TM half-life prolongs activity but reduces rapid reversibility [18], while increasing receptor-TM affinity does not necessarily improve cytotoxicity or cytokine release [19]. The covalent SpyCAR design shifts this balance toward stable loading. That may sustain activity at low free-TM concentrations, but withdrawal of TM may not immediately terminate signaling from already armed receptors. Changes in CD69/CD25 expression, cytokine secretion, and cytotoxicity following removal of free TM were not evaluated. Because SpyTag/SpyCatcher coupling is covalent, removal of free TM may not immediately terminate signaling from TM-loaded receptors; therefore, the present findings do not establish functional reversibility or rapid switching.

The complete SpyCAR-T/Raji/TM condition increased CD25 expression to 13.5%, whereas the control groups remained near baseline. Its lower magnitude com-

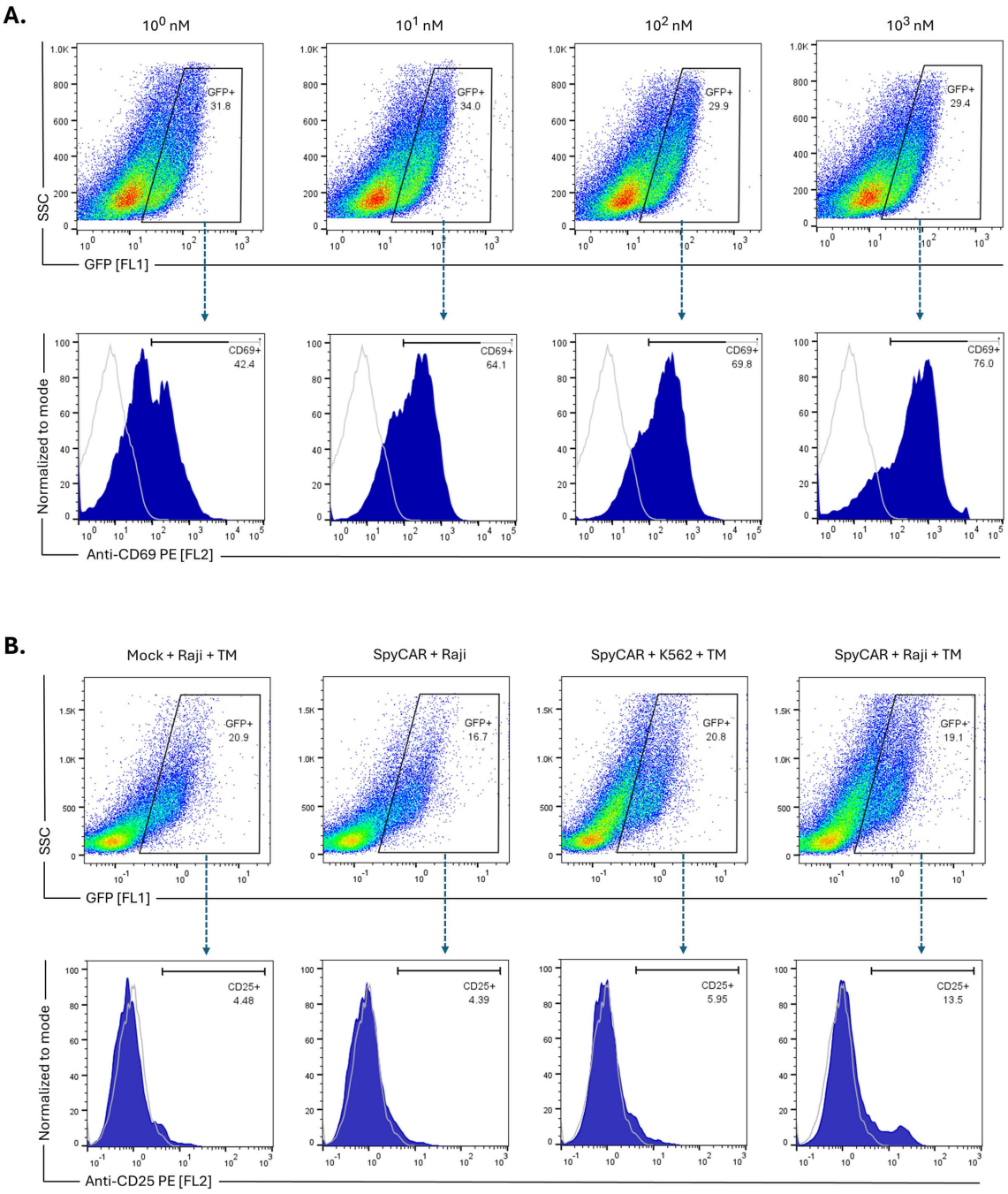


Fig. 2. TM-dependent activation of SpyCAR-T cells in the presence of CD22$^+$ target cells. (A) Flow-cytometric evaluation of the early T-cell activation marker CD69 in GFP$^+$ SpyCAR-T cells cocultured with CD22$^+$ Raji cells in the presence of increasing concentrations of the TM. CD69$^+$ cells accounted for 42.4%, 64.1%, 69.8%, and 76.0% of the GFP$^+$ population at TM concentrations of 1, 10, 100, and 1000 nM, respectively. A concentration of 10 nM was selected as the working concentration for subsequent functional experiments. (B) Evaluation of the late activation marker CD25 in different coculture conditions. CD25 positivity was 4.48% in mock-T cells cocultured with Raji cells and the TM, 4.39% in SpyCAR-T cells cocultured with Raji cells in the absence of the TM, and 5.95% in SpyCAR-T cells cocultured with CD22$^-$ K562 cells and the TM. In contrast, coculture of SpyCAR-T cells with CD22$^+$ Raji cells in the presence of the TM increased CD25 expression to 13.5%, consistent with a modest increase in CD25 positivity in the complete condition, although these data alone do not establish the specificity or robustness of the activation response. CD69 and CD25 expression was analyzed within the GFP$^+$ effector-cell gate. Gray histogram overlays represent unstained controls. Data are presented as mean ± SD from three separate experimental runs using cells from a single healthy donor. These represent within-donor experimental replicates rather than independent biological replicates.

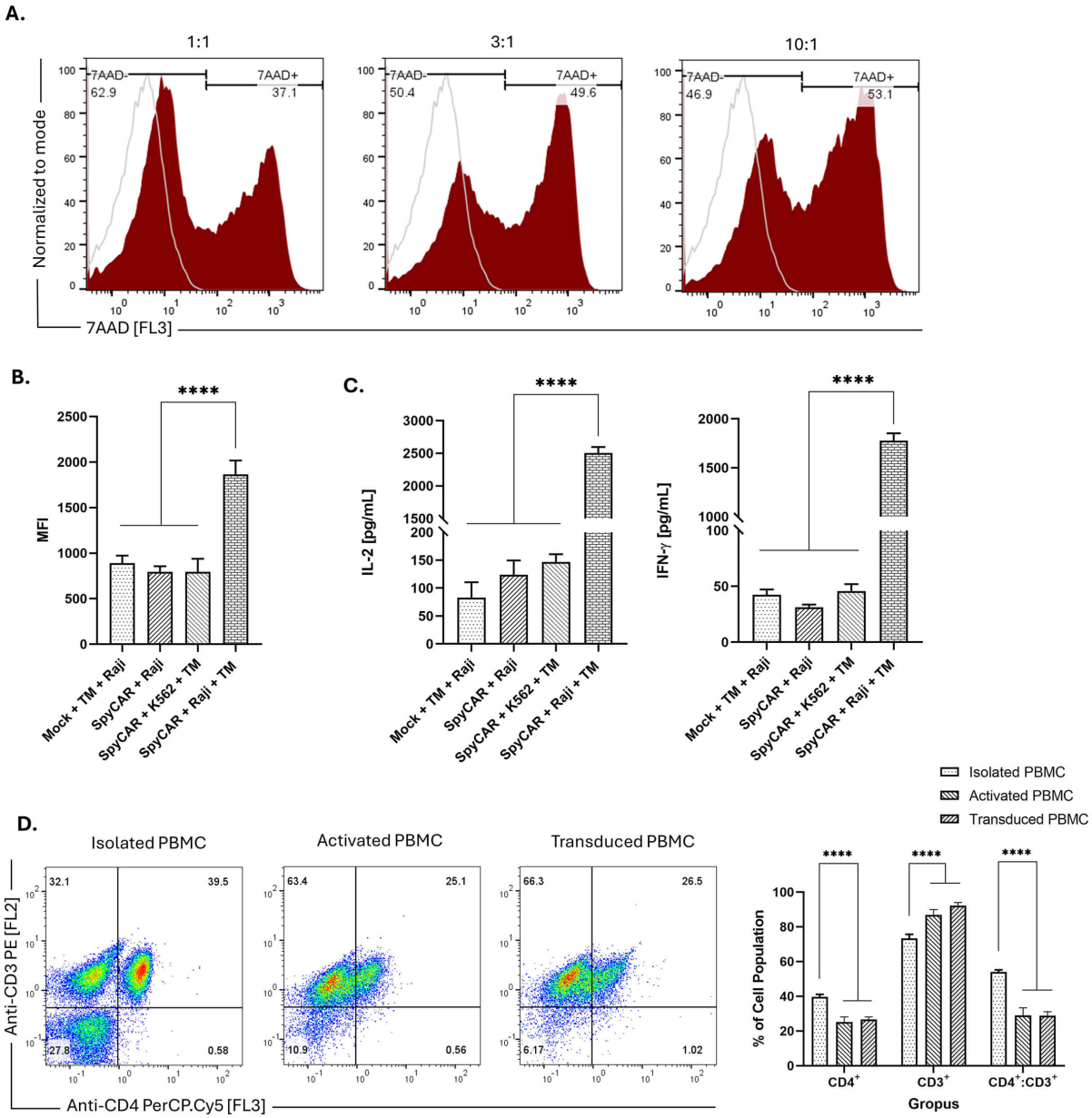


Fig. 3. Cytotoxicity, proliferation, cytokine secretion, and immunophenotypic characterization of SpyCAR-T cells. (A) Flow-cytometric evaluation of target-cell death following 24 h coculture of SpyCAR-T cells with $CD22^+$ target cells in the presence of 10 nM TM at effector-to-target (E:T) ratios of 1:1, 3:1, and 10:1. The percentages of 7-AAD^+ cells within the $CD3^-$ target-cell population were 37.17 ± 3.40%, 49.70 ± 3.75%, and 52.37 ± 6.53%, respectively. Because increasing the E:T ratio from 3:1 to 10:1 did not produce a significant additional cytotoxic effect, the 3:1 ratio was selected for subsequent functional assays. (B) Proliferative response of SpyCAR-T cells assessed by intracellular Ki-67 staining after 48 h of coculture. Ki-67 mean fluorescence intensity was markedly increased when SpyCAR-T cells were cocultured with $CD22^+$ Raji cells in the presence of the TM compared with the mock-T cell, TM-negative, and $CD22^-$ K562 control conditions. Error bars show mean ± SD. (C) Secretion of IL-2 and IFN-γ into coculture supernatants. SpyCAR-T cells cocultured with Raji cells in the presence of the TM produced 2506 ± 91.43 pg/mL IL-2 and 1777 ± 75.55 pg/mL IFN-γ, whereas cytokine secretion remained low in all control conditions. Data are presented as mean ± SD. (D) Flow-cytometric immunophenotyping of PBMCs immediately after isolation, following CD2/CD3/CD28-mediated activation, and 72 h after lentiviral transduction. $CD3^+$ cells were enriched following activation and remained predominant after transduction. Lentiviral transduction did not substantially alter the $CD4^+$ fraction within the $CD3^+$ T-cell population. Representative CD3/CD4 dot plots and the corresponding quantitative comparison of $CD4^+$, $CD3^+$, and $CD4^+/CD3^+$ populations are shown. Data are presented as mean ± SD from three separate experimental runs using cells from a single healthy donor. The replicates reflect within-donor experimental variability rather than between-donor variability. Error bars show mean ± SD. **** indicates $p < 0.0001$.

pared with CD69 is biologically plausible. CD69 is an early and sensitive activation marker, while CD25 reflects later and more sustained signaling and may be influenced by IL-2 production, consumption, receptor expression, and the differentiation state of the T cells. The two readouts are therefore complementary rather than contradictory. The modest CD25-positive fraction may partly reflect the different sampling times and readouts: CD25 was assessed at 24 h, whereas cytokine secretion and Ki-67 expression were evaluated at 48 h. Cytokine concentrations reflect accumulation in the culture supernatant, while CD25 positivity represents the fraction of cells exceeding a staining threshold at a single time point. These measurements therefore need not increase proportionally. However, the present data do not establish the cause of the modest CD25 response. Increased Ki-67 intensity and secretion of IL-2 at 2506 ± 91.43 pg/mL and IFN-γ at 1777 ± 75.55 pg/mL further support productive signaling. However, Ki-67 indicates cell-cycle engagement rather than completed cell divisions, and absolute cytokine concentrations should not be compared directly across studies because donor composition, CAR frequency, target burden, culture duration, and assay platforms differ. The activation findings remain preliminary, particularly given the modest CD25 response and single-donor design, and require confirmation in additional independent experiments and donors.

Cytotoxicity increased from 37.17 ± 3.40% at an E:T ratio of 1:1 to 49.70 ± 3.75% at 3:1 and 52.37 ± 6.53% at 10:1. These values represent the total proportion of dead target cells, defined as 7-AAD^{+} cells within the CD3^{-} population, and may therefore include a component of spontaneous or background target-cell death. Because background death in the corresponding control conditions was not subtracted, these values should not be interpreted as background-corrected specific lysis. Nevertheless, the relatively small increase in total target-cell death between E:T ratios of 3:1 and 10:1 suggests that cytotoxic activity approached an apparent plateau within 24 h, supporting the selection of the 3:1 ratio for subsequent assays. However, it does not establish the product's maximal cytolytic capacity. Because 7-AAD positivity was measured within CD3^{-} cells, the result represents target-cell death in the coculture rather than background-corrected specific lysis. Future analyses should subtract spontaneous target-cell death and include mock, TM-negative, and antigen-negative conditions at every E:T ratio. Serial-killing assays would also determine whether the observed plateau reflects target saturation, limited effector-cell recycling, receptor internalization, or early functional exhaustion. Because GFP expression in effector cells occupied one fluorescence channel and no additional target-specific labeling system was available, cytotoxicity was assessed within the CD3-negative population, which may include residual CD3-negative non-target cells and therefore limits the specificity of target-cell death measurements.

CD22 is clinically relevant because CD22-directed CAR-T cells have induced remissions in B-ALL, including disease resistant to CD19-directed therapy [20,21,22]. CAR activity depends strongly on antigen density [23], while CD22 is generally less abundant than CD19 and has a large extracellular domain that may constrain immune-synapse geometry [24]. The response against Raji cells is therefore encouraging but cannot be extrapolated directly to primary CD22^{low} leukemia. Raji and K562 are also not isogenic controls; they differ in adhesion molecules, accessory ligands, intracellular signaling, and intrinsic susceptibility to killing. CombiCell experiments showed that CAR sensitivity can be modified by accessory interactions, particularly LFA-1/ICAM-1, and that CARs remain less antigen-sensitive than native TCRs [25]. Thus, the K562 comparison supports antigen dependence but does not establish CD22 as the only variable responsible for the difference. CD22-knockout Raji cells, CD22-engineered K562 cells, and matched antigen-density panels would provide substantially stronger mechanistic evidence.

The broader value of a universal receptor lies in multiantigen control. Dual CD19/CD22 CAR studies indicate that two-antigen targeting can reduce antigen-negative escape, but also demonstrate the difficulty of achieving equivalent potency against both targets [26]. Cotransduced CD19/CD22 CAR-T cells reduced antigen-negative relapse, although limited cellular persistence remained a cause of treatment failure [27]. CD22 CAR-T cells engineered to secrete a CD19 T-cell engager have more recently improved control of heterogeneous B-ALL models [28]. SpyCAR offers a distinct strategy: one signaling-cell product could theoretically receive sequential or simultaneous SpyTagged TMs without further genetic modification. This potential advantage remains unproven in the current study and should be tested in mixed antigen-positive and antigen-negative populations, with sequential module exchange, simultaneous loading, competition experiments, and repeated exposure to antigenically heterogeneous targets.

Overall, the findings establish a credible proof of concept: a SpyCatcher-based CD28-CD3ζ receptor can be redirected by an anti-CD22 nanobody-SpyTag module to induce activation, proliferation-associated signaling, cytokine secretion, and preliminary cytotoxic activity against Raji Burkitt lymphoma cells *in vitro*. The decisive next steps are mechanistic studies of antigen-density thresholds, TM geometry and valency, functional reversibility, multiantigen retargeting, and efficacy in primary B-ALL samples and relevant *in vivo* models. Although experiments were performed in three separate runs, all cells originated from one donor. The statistical comparisons therefore reflect within-donor experimental variability and do not establish reproducibility across donors.

5. Limitations

This study provides an *in vitro* proof of concept using cells from one healthy donor. Although functional experiments were performed in three separate runs, these represent within-donor experimental replication and do not capture between-donor biological variability. The findings therefore require validation in additional donors. Experiments used established cell lines (target cells) rather than primary patient samples, and no animal studies were performed, limiting extrapolation to clinical settings.

No direct comparisons with a conventional anti-CD22 CAR, a noncovalent adaptor CAR, or a bond-deficient SpyTag/SpyCatcher control were included. Cytotoxicity was assessed as 7-AAD positivity within the CD3-negative coculture population without target-specific labeling or subtraction of spontaneous target-cell death.

6. Conclusion

This study establishes a proof of concept for a SpyTag/SpyCatcher-based universal CAR-T-cell platform capable of being redirected against CD22-expressing malignant cells through a SpyTag-fused anti-CD22 nanobody TM. The SpyCatcher-containing CAR was successfully expressed on the surface of primary human T cells and retained the predicted structural integrity required for TM engagement. In the simultaneous presence of the CD22-specific TM and $CD22^{+}$ target cells, SpyCAR-T cells exhibited coordinated and activation, proliferation, cytokine secretion, and cytotoxic activity, whereas these responses remained limited under the corresponding control conditions. The findings highlight the principal advantage of this platform: separation of antigen recognition from intracellular T-cell signaling, allowing a single engineered T-cell product to be theoretically redirected toward different tumor antigens by exchanging the TM. The absence of direct comparisons with a conventional anti-CD22 CAR, a noncovalent adaptor CAR, and a bond-deficient SpyTag/SpyCatcher control limits conclusions about comparative efficacy and the specific contribution of covalent coupling. Further development should focus on optimizing receptor and TM geometry, improving activity against CD22-low leukemia cells, evaluating simultaneous or sequential multi-antigen targeting, and defining TM occupancy and withdrawal kinetics. Validation in multiple donors, primary leukemia samples, and relevant *in vivo* models will also be essential. Overall, the SpyCAR platform represents a promising modular strategy for developing flexible and adaptable cellular immunotherapies for antigen-heterogeneous B-cell malignancies.

Availability of Data and Materials

The datasets used and analyzed during the current study are available from the corresponding authors on reasonable request.

Author Contributions

AM performed the main experimental work and drafted the manuscript. SA contributed to the design of the genetic construct and provided advice on assay design. MHA participated in designing the research study, focusing on the nanobody platform. AN and MJ participated in flow cytometry assays. AA supervised the research, contributed to the design of the SpyTag/SpyCatcher system, and critically revised the manuscript. ZS conceived and designed the study, supervised the research, and critically revised the manuscript. All authors contributed to editorial changes in the manuscript. All authors read and approved the final manuscript. All authors have participated sufficiently in the work and agreed to be accountable for all aspects of the work.

Ethics Approval and Consent to Participate

This study was approved by the Ethics Committee of the Pasteur Institute of Iran, Tehran, Iran, under approval code IR.PII.REC.1400.073. The study was carried out in accordance with the guidelines of the Declaration of Helsinki. Written informed consent was obtained from the healthy donor prior to blood sample collection and participation in the study.

Acknowledgment

The authors sincerely thank Dr. Farhad Riazi-Rad for his valuable support throughout the study.

Funding

This work was conducted as part of research project at Pasteur Institute of Iran [approval code: BP-98103].

Conflicts of Interest

The authors declare no conflicts of interest.

Declaration of AI and AI-Assisted Technologies in the Writing Process

During the preparation of this manuscript, the authors used ChatGPT-5.6 (OpenAI) to assist with cross-checking the consistency of the reported data, scientific rewriting of selected sections, and language and grammatical editing. The tool was not used to generate experimental data, perform statistical analyses, interpret results independently, or make scientific conclusions. All AI-assisted content was critically reviewed, verified, and revised by the authors, who take full responsibility for the accuracy, integrity, and final content of the manuscript.

Supplementary Material

Supplementary material associated with this article can be found, in the online version, at https://doi.org/10.31083/FBL57602.

References

[1] Akatsu C, Naito-Matsui Y, Abdu-Allah HHM, Imamura A, Long W, Ishida H, et al. Neu5Gc-mediated high-affinity interaction is dispensable for CD22 cis-ligands to regulate B cell signaling. Journal of Biological Chemistry. 2024; 300: 107630. https://doi.org/10.1016/j.jbc.2024.107630

[2] Testa U, Sica S, Pelosi E, Castelli G, Leone G. CAR-T Cell Therapy in B-Cell Acute Lymphoblastic Leukemia. Mediterranean Journal of Hematology and Infectious Diseases. 2024; 16: e2024010. https://doi.org/10.4084/MJHID.2024.010

[3] Lu Y, Zhao F. Strategies to overcome tumour relapse caused by antigen escape after CAR T therapy. Molecular Cancer. 2025; 24: 126. https://doi.org/10.1186/s12943-025-02334-6

[4] Minutolo NG, Sharma P, Poussin M, Shaw LC, Brown DP, Hollander EE, et al. Quantitative Control of Gene-Engineered T-Cell Activity through the Covalent Attachment of Targeting Ligands to a Universal Immune Receptor. Journal of the American Chemical Society. 2020; 142: 6554–6568. https://doi.org/10.1021/jacs.9b11622

[5] Hatlem D, Trunk T, Linke D, Leo JC. Catching a SPY: Using the SpyCatcher-SpyTag and Related Systems for Labeling and Localizing Bacterial Proteins. International Journal of Molecular Sciences. 2019; 20: 2129. https://doi.org/10.3390/ijms20092129

[6] Abdureheman T, Zhou H, Yang LT, Huang XS, Jing JJ, Duan CW, et al. Construction of Switch Modules for CAR-T Cell Treatment Using a Site-Specific Conjugation System. Bioconjugate Chemistry. 2024; 35: 604–615. https://doi.org/10.1021/acs.bioconjchem.4c00050

[7] Liu H, Liu X, Zhou X, Duan S, Huang X, Fei H, et al. Application of nanobody-based CAR-T in tumor immunotherapy (Review). International Journal of Molecular Medicine. 2025; 56: 187. https://doi.org/10.3892/ijmm.2025.5628

[8] Rahbarizadeh F, Ahmadvand D, Sharifzadeh Z. Nanobody; an old concept and new vehicle for immunotargeting. Immunological Investigations. 2011; 40: 299–338. https://doi.org/10.3109/08820139.2010.542228

[9] Kim J, Sang Z, Xiang Y, Shen Z, Shi Y. Nanobodies: Robust miniprotein binders in biomedicine. Advanced Drug Delivery Reviews. 2023;195:114726. https://doi.org/10.1016/j.addr.2023.114726

[10] Maali A, Gholizadeh M, Feghhi-Najafabadi S, Noei A, Seyed-Motahari SS, Mansoori S, et al. Nanobodies in cell-mediated immunotherapy: On the road to fight cancer. Frontiers in Immunology. 2023; 14: 1012841. https://doi.org/10.3389/fimmu.2023.1012841

[11] Maali A, Abdoli S, Habibi-Anbouhi M, Noei A, Kadkhodazadeh M, Motamedirad M, et al. Development and Characterization of A Novel SpyTagged Modular Nanobody as A Detection Platform for CD22-Positive Cells. Cell Journal. 2024; 26: 487–495. https://doi.org/10.22074/cellj.2024.2028911.1573

[12] Zakeri B, Fierer JO, Celik E, Chittock EC, Schwarz-Linek U, Moy VT, et al. Peptide tag forming a rapid covalent bond to a protein, through engineering a bacterial adhesin. Proceedings of the National Academy of Sciences of the United States of America. 2012; 109: E690–E697. https://doi.org/10.1073/pnas.1115485109

[13] Guo C, Guo X, Li X, Dong M, Wang X, Cheng S, et al. The SpyCatcher-SpyTag interaction mediates tunable anti-tumor cytotoxicity of NK cells. Molecular Immunology. 2024; 165: 11–18. https://doi.org/10.1016/j.molimm.2023.12.001

[14] Cardle II, Scherer DR, Jensen MC, Pun SH, Sellers DL. In Situ Bioconjugation of Synthetic Peptides onto Universal Chimeric Antigen Receptor T Cells for Targeted Cancer Immunotherapies. ACS Nano. 2025; 19: 5750–5768. https://doi.org/10.1021/acsnano.4c16824

[15] An M, Wang Y, Shao J, Wu S, Yan J, Li Y, et al. Anti-MSLN chimeric antigen receptor-like NK cell therapy with tumor-penetrating capacity (uCAR-like NK) for solid tumors. Signal Transduction and Targeted Therapy. 2025; 10: 425. https://doi.org/10.1038/s41392-025-02524-0

[16] Loff S, Dietrich J, Meyer JE, Riewaldt J, Spehr J, von Bonin M, et al. Rapidly Switchable Universal CAR-T Cells for Treatment of CD123-Positive Leukemia. Molecular Therapy Oncolytics. 2020; 17: 408–420. https://doi.org/10.1016/j.omto.2020.04.009

[17] Wermke M, Kraus S, Ehninger A, Bargou RC, Goebeler ME, Middeke JM, et al. Proof of concept for a rapidly switchable universal CAR-T platform with UniCAR-T-CD123 in relapsed/refractory AML. Blood. 2021; 137: 3145–3148. https://doi.org/10.1182/blood.2020009759

[18] Loureiro LR, Feldmann A, Bergmann R, Koristka S, Berndt N, Máthé D, et al. Extended half-life target module for sustainable UniCAR T-cell treatment of STn-expressing cancers. Journal of Experimental & Clinical Cancer Research: CR. 2020; 39: 77. https://doi.org/10.1186/s13046-020-01572-4

[19] Boutier H, Loureiro LR, Hoffmann L, Arndt C, Bartsch T, Feldmann A, et al. UniCAR T-Cell Potency-A Matter of Affinity between Adaptor Molecules and Adaptor CAR T-Cells? International Journal of Molecular Sciences. 2024; 25: 7242. https://doi.org/10.3390/ijms25137242

[20] Fry TJ, Shah NN, Orentas RJ, Stetler-Stevenson M, Yuan CM, Ramakrishna S, et al. CD22-targeted CAR T cells induce remission in B-ALL that is naive or resistant to CD19-targeted CAR immunotherapy. Nature Medicine. 2018; 24: 20–28. https://doi.org/10.1038/nm.4441

[21] Pan J, Niu Q, Deng B, Liu S, Wu T, Gao Z, et al. CD22 CAR T-cell therapy in refractory or relapsed B acute lymphoblastic leukemia. Leukemia. 2019; 33: 2854–2866. https://doi.org/10.1038/s41375-019-0488-7

[22] Shah NN, Highfill SL, Shalabi H, Yates B, Jin J, Wolters PL, et al. CD4/CD8 T-Cell Selection Affects Chimeric Antigen Receptor (CAR) T-Cell Potency and Toxicity: Updated Results From a Phase I Anti-CD22 CAR T-Cell Trial. Journal of Clinical Oncology. 2020; 38: 1938–1950. https://doi.org/10.1200/JCO.19.03279

[23] Majzner RG, Rietberg SP, Sotillo E, Dong R, Vachharajani VT, Labanieh L, et al. Tuning the Antigen Density Requirement for CAR T-cell Activity. Cancer Discovery. 2020; 10: 702–723. https://doi.org/10.1158/2159-8290.CD-19-0945

[24] Kokalaki E, Ma B, Ferrari M, Grothier T, Hazelton W, Manzoor S, et al. Dual targeting of CD19 and CD22 against B-ALL using a novel high-sensitivity aCD22 CAR. Molecular Therapy. 2023; 31: 2089–2104. https://doi.org/10.1016/j.ymthe.2023.03.020

[25] Patel A, Andre V, Eguiguren SB, Barton MI, Burton J, Denham EM, et al. Using CombiCells, a platform for titration and combinatorial display of cell surface ligands, to study T-cell antigen sensitivity modulation by accessory receptors. The EMBO Journal. 2024; 43: 132–150. https://doi.org/10.1038/s44318-023-00012-1

[26] Spiegel JY, Patel S, Muffly L, Hossain NM, Oak J, Baird JH, et al. CAR T cells with dual targeting of CD19 and CD22 in adult patients with recurrent or refractory B cell malignancies: a phase 1 trial. Nature Medicine. 2021; 27: 1419–1431. https://doi.org/10.1038/s41591-021-01436-0

[27] Ghorashian S, Lucchini G, Richardson R, Nguyen K, Terris C, Guvenel A, et al. CD19/CD22 targeting with cotransduced CAR T cells to prevent antigen-negative relapse after CAR T-cell therapy for B-cell ALL. Blood. 2024; 143: 118–123. https://doi.org/10.1182/blood.2023020621

[28] Arroyo-Ródenas J, Falgas A, Díez-Alonso L, Martinez-Moreno A, Roca-Ho H, Gil-Etayo FJ, et al. CD22 CAR-T cells secreting CD19 T-cell engagers for improved control of B-cell acute lymphoblastic leukemia progression. Journal for Immunotherapy of Cancer. 2025; 13: e009048. https://doi.org/10.1136/jitc-2024-009048